Electronic Supplementary Information

Stirring hydrothermal synthesis of ultra long α-MnO_2 nanowires for oxygen reduction reaction

Kaixiang Lei[a†], Liang Cong[a†], Xiaorui Fu[a], Fangyi Cheng[a]* and Jun Chen[a,b]

[a] *Key Laboratory of Advanced Energy Materials Chemistry (Ministry of Education), College of Chemistry,* [b] *Collaborative Innovation Center of Chemical Science and Engineering, Nankai University, Tianjin 300071, China*

E-mail: fycheng@nankai.edu.cn. Fax: +86-22-23509571. Tel: +86-22-23497717.

†These authors contribute equally to this work.

Experimental

Synthesis

The preparation of ultra long MnO_2 nanowires involves two steps: synthesis of MnO_x intermediate through hydrothermal with stirring, and heat treatment of MnO_x in air. Briefly, 100 mg of commercial MnO_2 powders was dispersed into 20 ml of $NH_3 \cdot H_2O$ solution. After continuous stirring for 10 min, the above-mentioned mixture was transferred into a 50 ml Teflon-lined autoclave with a magnetic stirrer. Then, the autoclave was loaded into a silicon oil bath on a hot plate. The synthesis was optimized by adjusting reaction temperature, concentration of $NH_3 \cdot H_2O$ solution, and reaction time. After being cooled to

room temperature, the as-obtained precipitates were centrifuged, washed with deionized water and absolute alcohol and finally vacuum-dried at 80 ^{o}C overnight. The intermediate was calcined at 300 ^{o}C for 1 h in air to obtain ultra long MnO_2 nanowires. For comparison, similar procedures were used to prepare MnO_x nanorods/nanowires with no or weak magnetic stirring. Table S1 lists the typical synthetic parameters.

Table S1 Synthetic parameters for MnO_x samples.

Stirring	**$NH_3 \cdot H_2O$ Concentration (mol L^{-1})**	**Time (h)**	**Temperature (^{o}C)**
strong	0.5	12	120
strong	0.5	12	140
strong	0.5	12	160
strong	2	12	160
strong	4	1	160
strong	4	12	160
strong	4	24	160
strong	4	48	160
weak	4	48	160
strong	4	48	180
strong	4	48	140
strong	4	48	120

Material characterization

The as-synthesized samples were characterized with power X-ray diffraction (XRD) on a Rigaku X-2500 diffractometer using Cu Kα radiation at a scanning speed of 4° min^{-1} from 10° to 80°, scanning electron microscopy (SEM, JEOL JSM-7500F), transmission electron microscopy (TEM, Philips Tecnai F20), X-ray photoelectron spectroscopy (XPS, Perkin Elmer PHI 1600 ESCA system), and N_2 adsorption/desorption measurement (BEL Sorp mini). Electrical conductivity measurements were conducted by pressing the materials into chips between two stainless steel electrodes and measuring the resistance of the respective sample by ohm's law on Ametek Parstat 4000. The conductivity κ was calculated using the equation: $\kappa = 1/\rho = h/(R*S)$, where ρ is resistivity, S and h are the surface area and thickness of the chips, respectivity.

Electrode preparation

The samples (3 mg) were mixed with carbon powders (7 mg, Carbon Vulcan XC-72), isopropanol (950 μL), Nafion (50 μL, 5 wt.%, Sigma-Aldrich). The carbon powders were used to improve the electronic conductivity. The ratio between manganese oxides and Vc-72 is 3:7. Then, this mixture was ultrasonicated for 30 min to make a homogenous ink. Finally, 7 μL of the obtained suspension was loaded on a glassy carbon electrode (GCE, 5.61 mm, diameter) and dried for 8 h under isopropanol atmosphere at room temperature. The electrochemical

performance was compared with carbon-supported Pt nanoparticles (Pt/C, the Pt loading is around 20 wt%).

Electrochemical tests

A standard three-electrode cell was used to test the electrochemical performance at room temperature. Saturated calomel electrode (SCE) and Pt foil were served as the reference electrode and counter electrode, respectively. The working electrode was GCE covered with a thin catalyst film. The following tests were conducted in 0.1 M aqueous KOH electrolyte saturated with high-purity O_2 or Ar and maintained under O_2 or Ar atmosphere during the test. The voltammetry was obtained at a potential scanning rate of 20 mV s^{-1}. The ORR polarization curves were collected using the catalyst-loaded rotation ring-disk electrode (RRDE) at different rotation rates and at a scan rate of 5 mV s^{-1}. Unless stated, all potentials in this paper are reported against RHE, E(RHE) = E(SCE) + 0.99 V.[S1] Based on LSV, the onset potential of ORR is determined by the point, where the current density for ORR is first observed (i.e., the current density falls below 0 mA cm^{-2}). The half-wave potential is the potential where the current halves the limiting current.

The overall electron transfer number can be calculated from the slope of Koutecky-Levich (K-L) plots (i^{-1} vs. $\omega^{-1/2}$) based on the K-L equation:

$$\frac{1}{i}=\frac{1}{i_k}+\frac{1}{i_d}=\frac{1}{nFAKC^0}-\frac{1}{0.62nFAD_{o_2}{}^{2/3}\nu^{-1/6}C^0\omega^{1/2}} \quad (1)$$

where i is the measured current density, i_k and i_d are the kinetic current and limiting current densities, ω is the angular velocity of the disk ($\omega = 2\pi N$, N is the rotation speed), n is the total number of electrons transferred in the ORR, F is the Faraday constant (F = 96500 C mol^{-1}), A is the geometric electrode area (cm^2), K is the rate constant of the reaction, C^0 is the saturated O_2 concentration in the electrolyte, D_{O2} is the diffusion coefficient of O_2, and v is the kinematic viscosity of the electrolyte. i_k is obtained from mass-diffusion correction according to the following equation:

$$i_k = \frac{i \times i_d}{i_d - i} \tag{2}$$

The electron transfer number (n) and the percentage of peroxide species relative to the total product (y) can be calculated through the following equation:

$$n = \frac{4Ni_d}{Ni_d + i_r} \tag{3}$$

$$y = \frac{200i_r}{Ni_d + i_r} \tag{4}$$

where N is the current efficiency of RRDE, and i_d and i_r are the disk and ring currents, respectively.

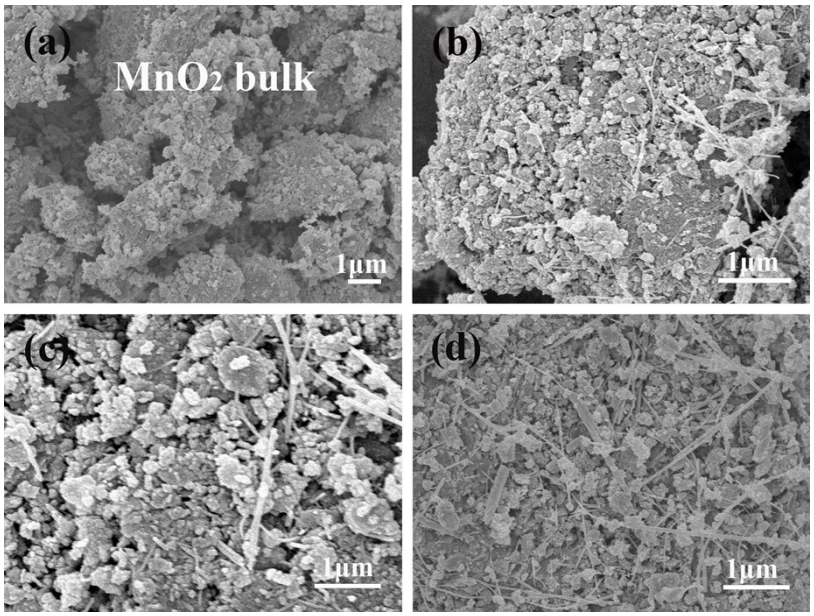

Fig. S1 SEM images of (a) MnO_2 bulk and (b-d) the intermediate MnO_x NWs at different temperature: (b) 120 °C, (c) 140 °C, and (d) 160 °C. $NH_3 \cdot H_2O$ concentrations 0.5 M, reaction time 12 h.

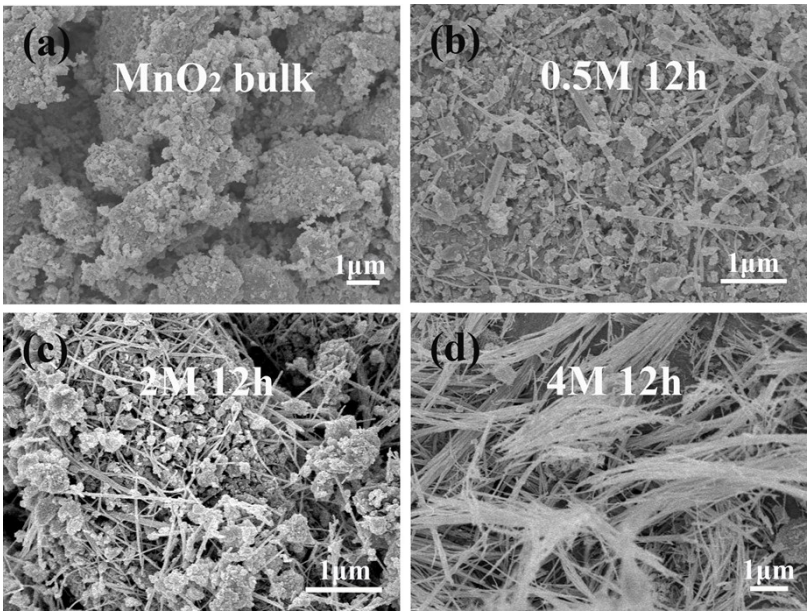

Fig. S2 SEM images of (a) MnO_2 bulk and (b-d) the intermediate MnO_x NWs at different $NH_3 \cdot H_2O$ concentrations: 0.5, 2, and 4 M. Temperature 160 °C, reaction time 12 h.

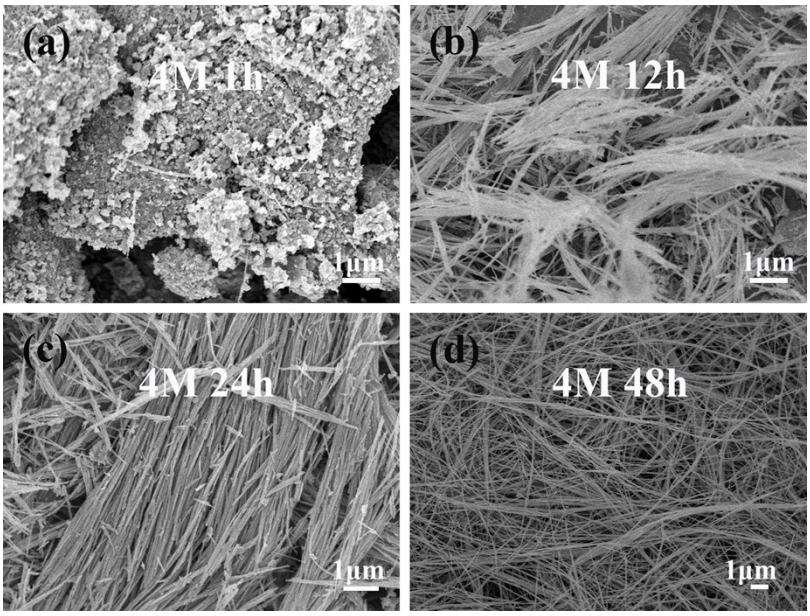

Fig. S3 SEM images of the intermediate MnO_x NWs synthesized with different reaction time: (a) 1, (b) 12, (c) 24, (d) 48 h. Temperature 160 ^oC, $NH_3 \cdot H_2O$ concentration 4 M.

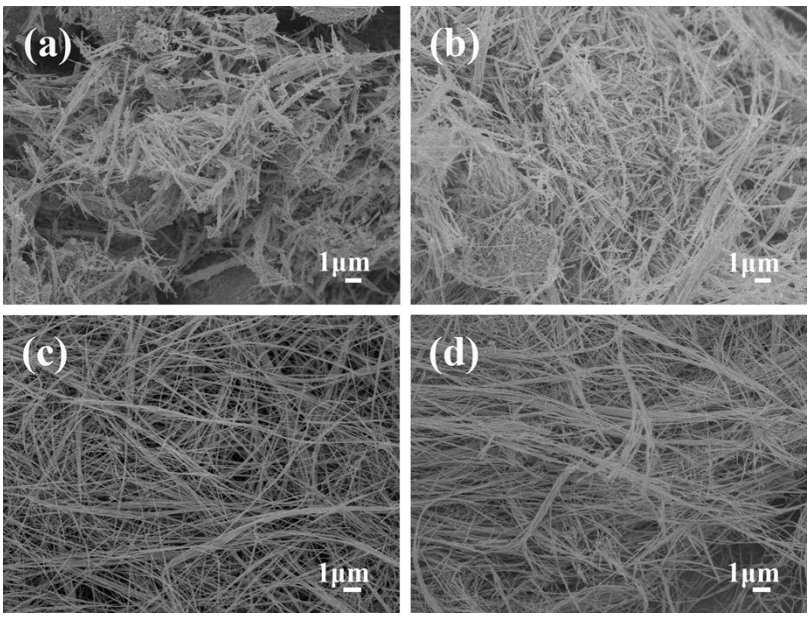

Fig. S4 SEM images of the intermediate MnO_x NWs at different temperature: (a) 120 ^oC, (b) 140 ^oC, (c) 160 ^oC, and (d) 180 ^oC. $NH_3 \cdot H_2O$ concentrations 4 M, reaction time 48 h.

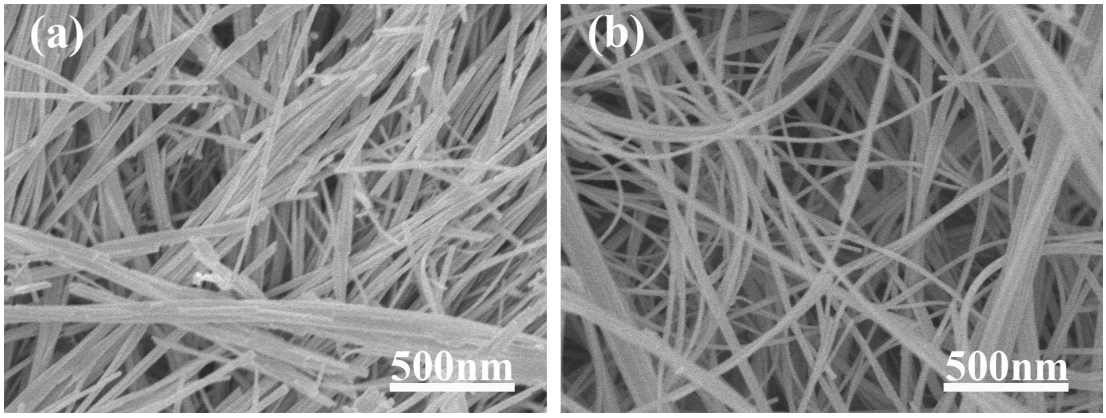

Fig. S5 SEM images of the intermediate MnO_x NWs obtained under (a) weak stirring and (b) strong stirring. Temperature 160 ^oC, $NH_3 \cdot H_2O$ concentrations 4 M, reaction time 48 h.

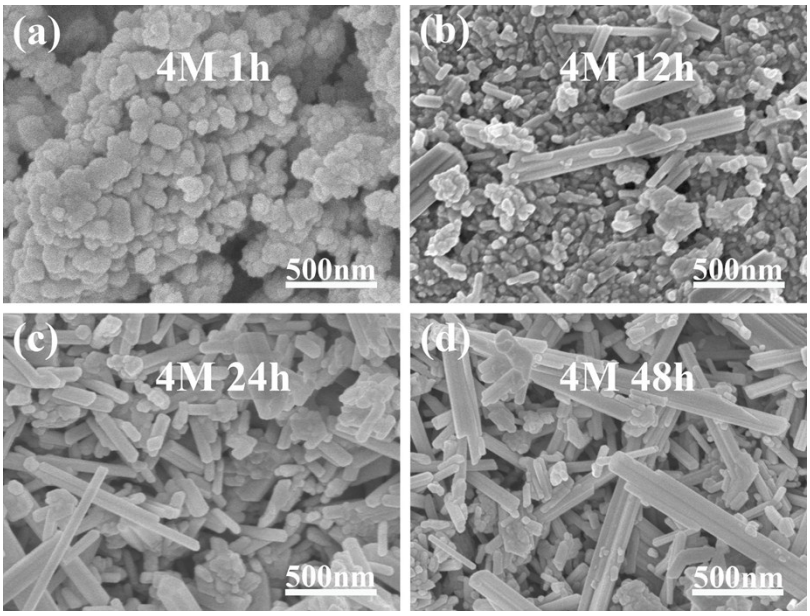

Fig. S6 SEM images of the intermediate MnO_x NRs synthesized without stirring at different reaction time: (a) 1, (b) 12, (c) 24, and (d) 48 h. Temperature 160 ^oC, $NH_3 \cdot H_2O$ concentration 4 M.

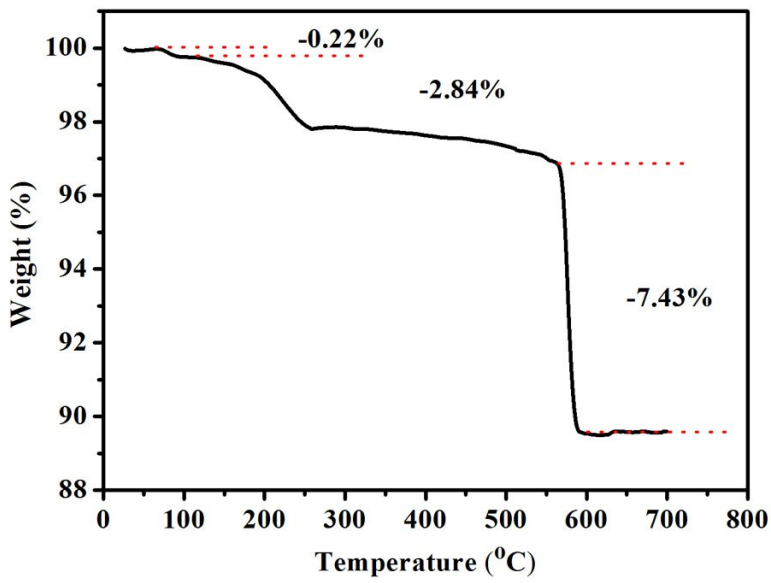

Fig. S7 TG curve of the as-synthesized intermediate MnO_x NWs in air at a heating rate of 10 °C min^{-1}.

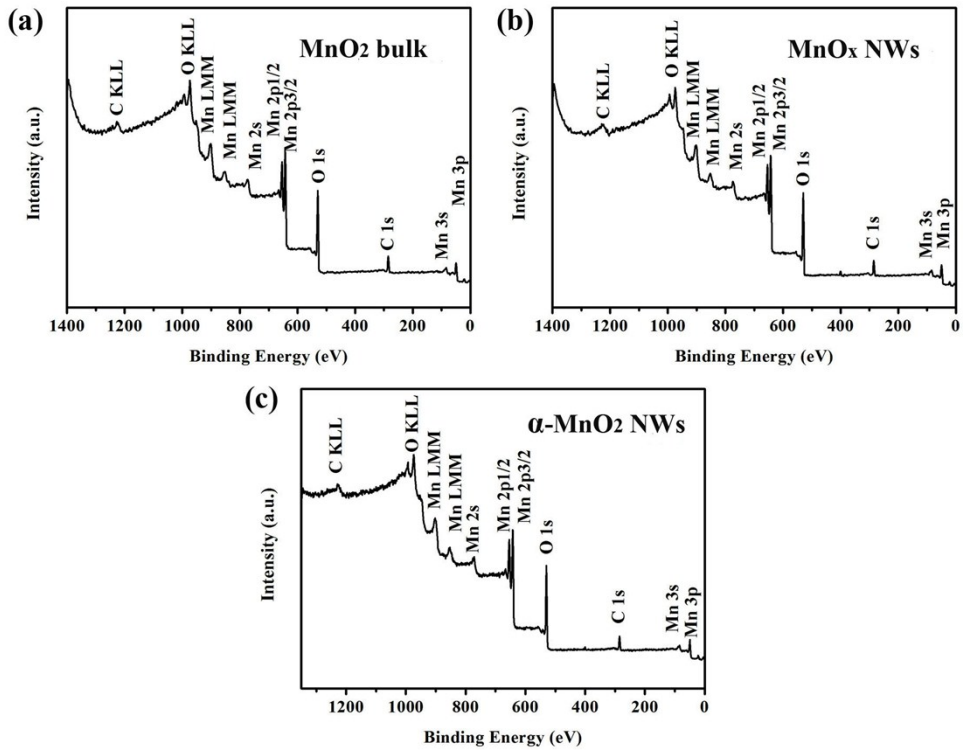

Fig. S8 XPS survey scan spectra of (a) MnO_2 bulk, (b) MnO_x NWs, and (c) α-MnO_2 NWs.

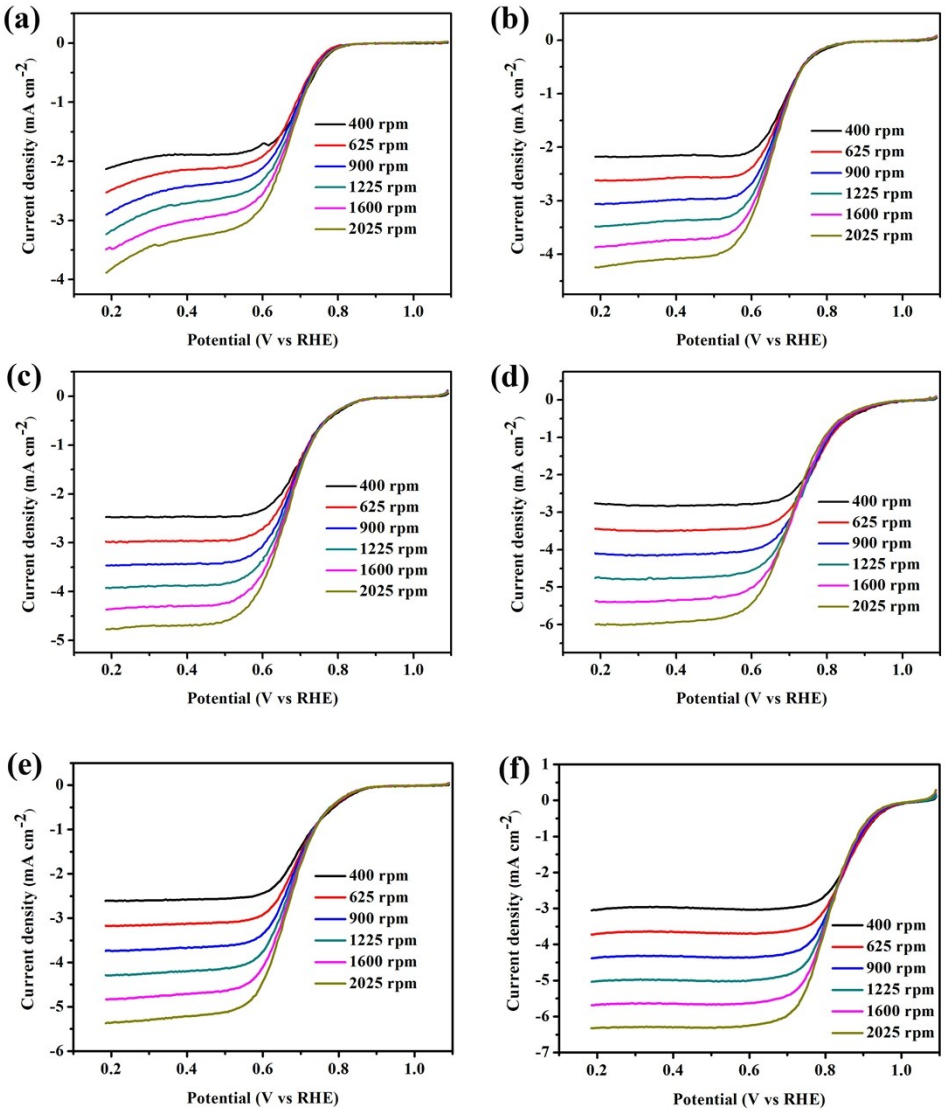

Fig. S9 LSVs of (a) Vc-72, (b) MnO_2 bulk, (c) MnO_x NWs, (d) α-MnO_2 NWs, (e) MnO_2 NRs, and (f) Pt/C recorded in O_2-saturated 0.1 M KOH solution.

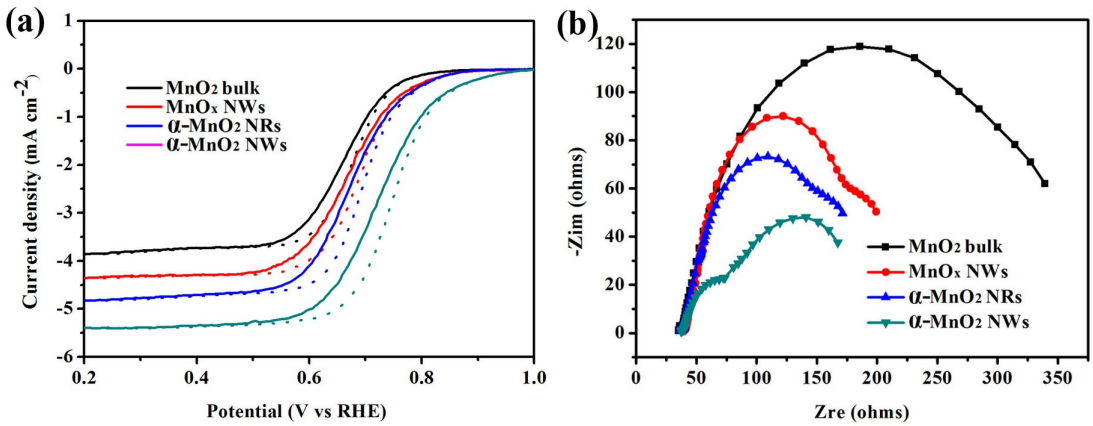

Fig. S10 (a) The polarization curves with (dotted line) and without iR-correction (solid line) of MnO_2 bulk MnO_x NWs, α-MnO_2 NRs, and α-MnO_2 NWs recorded at 1600 rpm in O_2-saturated 0.1 M KOH solution. (b) EIS spectroscopies of MnO_2 bulk, MnO_x NWs, α-MnO_2 NRs, and α-MnO_2 NWs.

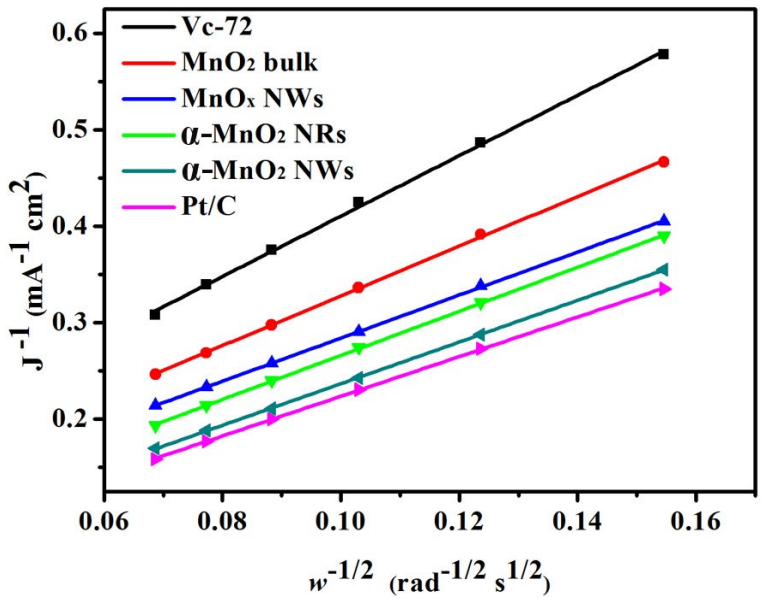

Fig. S11 K-L plots of different samples at 0.45 V.

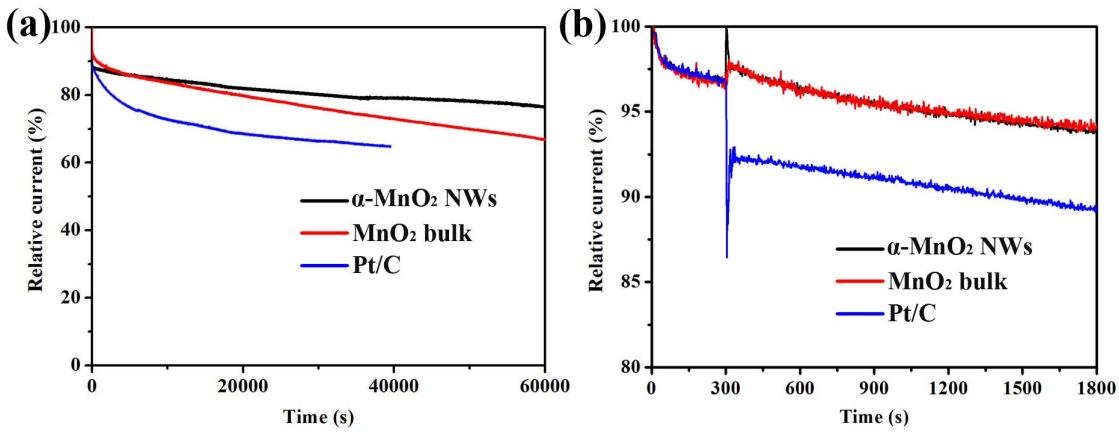

Fig. S12 Chronoamperometric curves of MnO_2 bulk, MnO_2 NWs, and Pt/C (a) in alkaline media; (b) after the introduction of 2.5 ml methanol into 200 ml of 0.1 M KOH solution.

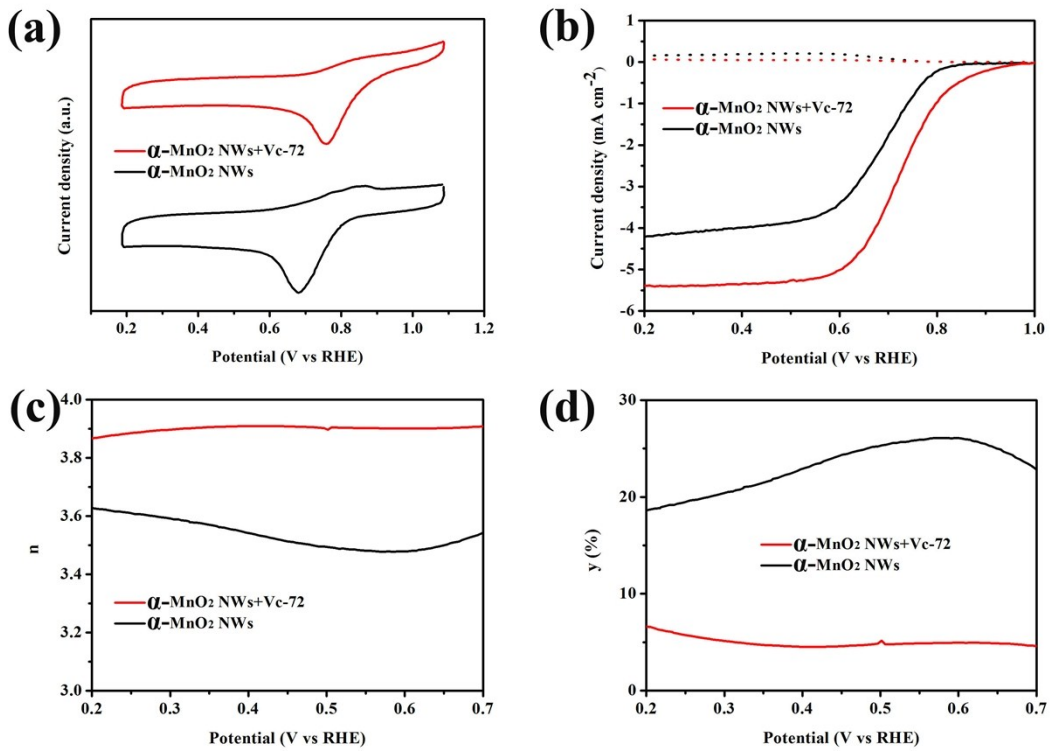

Fig. S13 The comparsion of electrochemical performance between α-MnO_2 NWs and α-MnO_2 NWs+Vc-72.

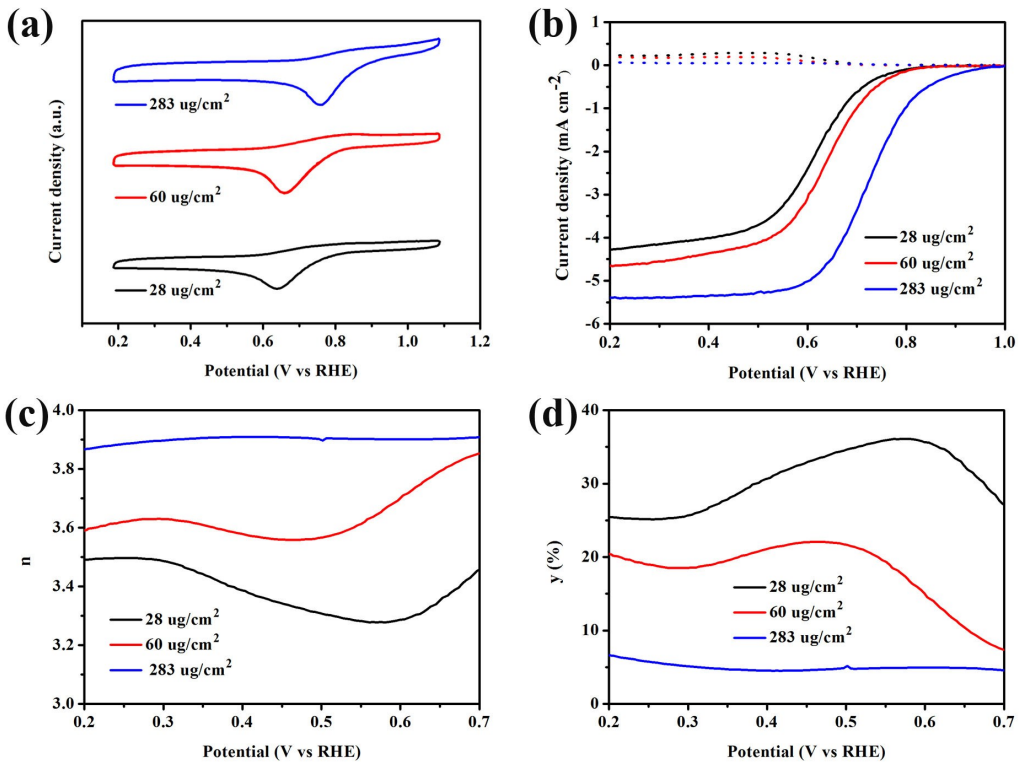

Fig. S14 The comparsion of electrochemical performance between among different loading of α-MnO_2 NWs containing Vc-72.

1 **Table S2** Some recently reported α-MnO_2 NWs as ORR catalysts[a]

Samples	E_{onset} (V)	E_{half} (V)	i_k (mA cm^{-2})	I_m (mA mg^{-1})	Ref
α-MnO_2 NWs	0.94	0.72	9.42	62.60	This work
α-MnO_2 nanorods	0.89	0.71	6.00	14.72	8c
α-MnO_2 nanotubes	0.89	0.70	3.00	14.72	8c
Ni-α-MnO_2 NWs/graphene	0.91	0.74	3.08	22.08	17b
Cu-α-MnO_2 NWs/graphene	0.95	0.74	4.00	23.56	17b
Cu-α-MnO_2 NWs	0.85	0.71	2.40	11.88	17e
MnO_2 nanorods with vacancies	0.86	0.72	9.48	72.60	19a
α-MnO_2 nanoparticles	0.71	0.57	0.11	22.19	30a
Long belt-like α-MnO_2	0.92	0.75	16	52.35	30b
α-MnO_2 NWs	0.89	0.64	1.93	28.57	30c

2 [a] E_{onset}, E_{half}, i_k, I_m, and n represent onset potential, half-wave potential, kinetic
3 current density, mass activity and electron transfer number, respectively. The
4 values of I_m and n are determined at 0.45 V. i_k is determined at 0.7 V.

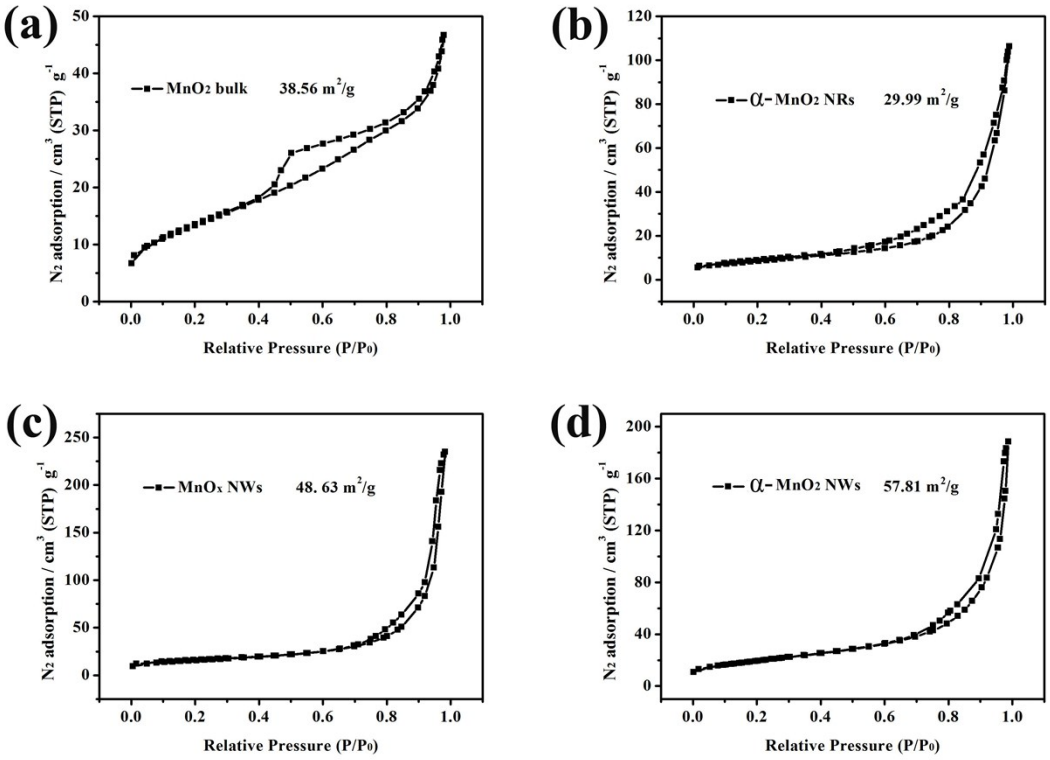

Fig. S15 N_2 sorption isotherms (measured at 77 K) of the as-synthesized materials.

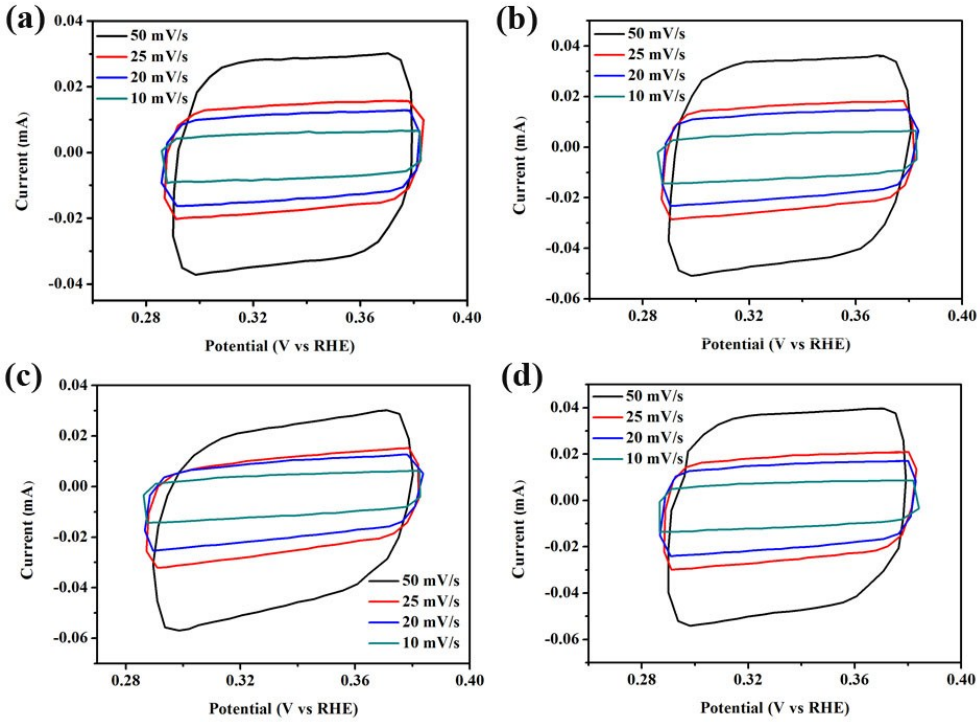

Fig. S16 CV curves with different scan rates between 290 and 390 mV for (a) MnO_2 bulk, (b) MnO_x NWs, (c) α-MnO_2 NRs, and (d) α-MnO_2 NWs.

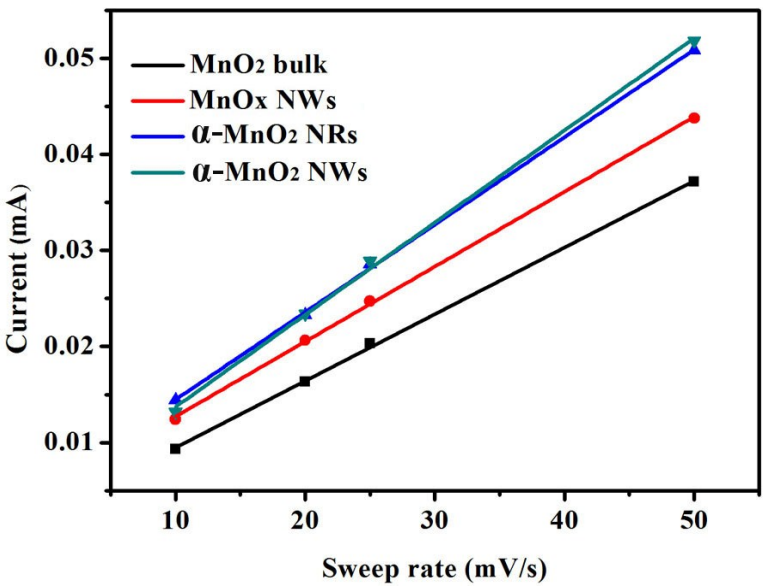

Fig. S17 Dependence of current as a function of scan rate at measured potential of 340 mV.

The electrochemical surface area (ECSA) was calculated from the Coulombic charge Q for hydrogen desorption based on the equation:[S2]

$$ECSA = \frac{Q}{m \times C} \quad (5)$$

where Q = S/v (S peak area, v scan rate). The ECSA of manganese oxides was estimated adopting an in stiu method on the basis of the measuement of double layer capacitance. In Ar, we found that the electrochemical response in the region of 0.29-0.39 V was dominated by the double layer capacitance without significant faradaic processes. The approximately rectangular shape of the cyclic voltammograms between 0.29 and 0.39 V and the linear relation between the current and the scan rate confirmed the absence of the faradaic processes. The ECSA was determined assuming a C_{dl} capacitance of 60 μF cm^{-2}.[S3] The obtained ECSA of MnO_2 bulk, MnO_x NWs, MnO_2 NRs, and MnO_2 NWs was 54.7, 60.6, 63.5, and 74.3 m^2/g, respectively.

Reference:

S1 (a) Y. Liang, Y. Li, H. Wang, J. Zhou, J. Wang, T. Regier and H. J. Dai, *Nat. Mater.,* 2011, **10**, 780. (b) X. Han, T. Zhang, J. Du, F. Cheng and J. Chen, *Chem. Sci.,* 2013, **4**, 368.

S2 T. J. Schimdt, H. A. Gasteiger, G. D. Stab, P. M. Urban, D. M. KoIb and R. J. Behm, *J. Electrochem. Soc.,* 1998, **145**, 2354.

S3 S. Levine, A. L. Smith, *Discuss. Faraday Soc.,* 1971, **52**, 290.